PERGAMON

International Journal of Solids and Structures 38 (2001) 8975–8987

INTERNATIONAL JOURNAL OF SOLIDS and STRUCTURES

www.elsevier.com/locate/ijsolstr

Analysis of large deflection equilibrium states of composite shells of revolution. Part 2. Applications and numerical results

Alexander Yu. Evkin, Alexander L. Kalamkarov *

Department of Mechanical Engineering, Smart Materials Centre, Dalhousie University, P.O. Box 1000, Halifax, Nova Scotia, Canada B3J 2X4

Received 17 February 2001; in revised form 3 August 2001

Abstract

The behavior of composite shells of revolution with large deflections (load–displacement diagrams and stress states) is studied. The nonlinear boundary value problems for composite shells of revolution, which have been obtained in Part 1 of the present study by means of the asymptotic approximation of Reissner's equations, are analyzed. The numerical solutions of these problems are obtained in several cases of a practical importance. The composite spherical shells with different types of boundary conditions as well as the completed orthotropic ellipsoids of revolution under uniform external pressure and concentrated load are considered in detail. The high accuracy and effectiveness of the obtained asymptotic solutions are demonstrated by means of comparing the asymptotic results with numerical solutions of the original Reissner's equations.

Keywords: Composite shell of revolution; Large deformations; Asymptotic solutions; Spherical and ellipsoidal composite shells

1. Introduction

The major practical problem in the analysis of behavior of shells with large deflections is to describe the load–displacement diagram of structures and to estimate their stress and strain equilibrium states. The direct application of numerical methods is very difficult because of a significant nonlinearity and singularity of the problems (Graff et al., 1985; Evkin and Korovaitsev, 1992; Korovaitsev and Evkin, 1992). Therefore, for these purposes we are using the asymptotic boundary value problems, which have been obtained in Part 1 of the present study (Evkin and Kalamkarov, 2001). These problems are significantly simpler compared with the original Reissner's equations (Reissner, 1969, 1972). Despite the attained simplicity, the level of accuracy of asymptotic equations has remained similar to the original one in the asymptotic sense.

According to the asymptotic approach we distinguish two types of the shell behavior. The first one corresponds to nonsmall values of load parameter, when the inner boundary layer is located close to the

* Corresponding author. Tel.: +1-902-494-6072; fax: +1-902-423-6711.
E-mail address: alex.kalamkarov@dal.ca (A.L. Kalamkarov).

0020-7683/01/$ - see front matter
PII: S0020-7683(01)00185-8

shell boundary and is interacted with it by reversing the structure. In this case, we will obtain in the present paper the numerical solutions for composite spherical shallow caps with different types of boundary conditions. This will allow us to illustrate the effectiveness of the approach, as well as to describe the particularities of the structure equilibrium states. The second type of the shell behavior with large deflections corresponds to the asymptotically small values of load parameter, and it occurs when the inner boundary layer is located far enough from the shell edge, or, for example, in the case of completed shells. The last problem is much simpler compared with the first one, because of its independence from boundary conditions. In this case, there is no need to solve a boundary value problem, and it is sufficient to apply the asymptotic formulae obtained in Part 1 of this study in order to analyze the behavior of thin orthotropic ellipsoids of revolution both under uniform external pressure and transversal force concentrated in the shell pole. We also compare asymptotic solutions with numerical results for the original boundary value problem in order to verify the accuracy of our asymptotic approach.

2. Axisymmetrical deformation of a thin composite spherical shell

In this section we analyze numerically the asymptotic boundary value problems which have been obtained in Part 1 of this study (Evkin and Kalamkarov, 2001). We will consider the case when the inner boundary layer is located close to the shell boundary with coordinate $\xi_* \approx \xi_0$ (Fig. 1). Therefore the main asymptotic equations (3.29) and (3.30) of Part 1 of the present study could be represented as follows:

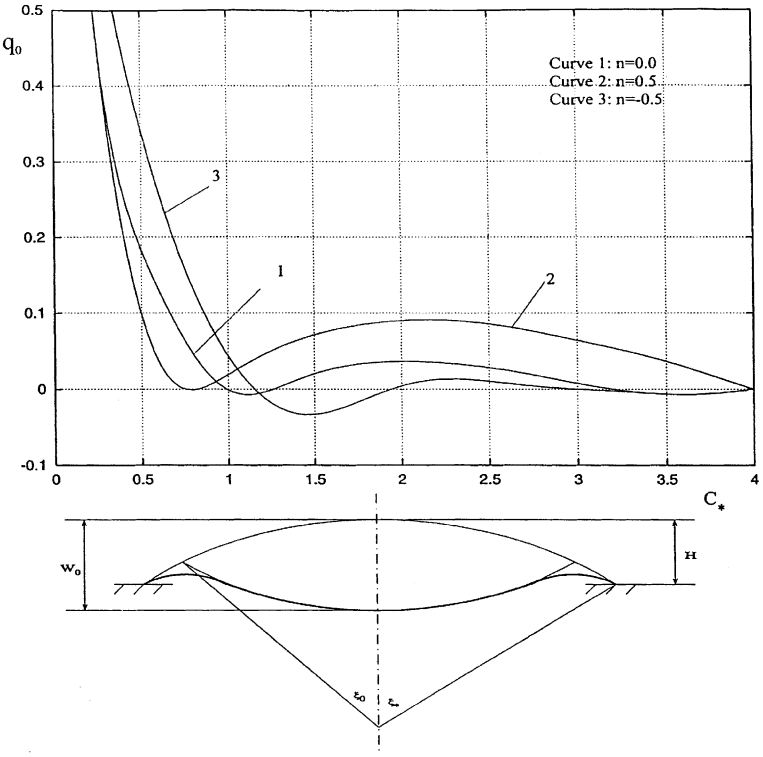

Fig. 1. Load parameter versus deflection amplitude of rigidly clamped composite cap.

$$\frac{d^2\psi}{d\xi^2} + \sin\xi_* n \frac{d^2\overline{U}}{d\xi^2} = \overline{U}\sin\psi + \hat{q}_v\cos\psi \tag{2.1}$$

$$\frac{d^2\overline{U}}{d\xi^2} - \frac{n}{\sin\xi_*}\frac{d^2\psi}{d\xi^2} = \frac{\cos\psi - \cos\xi_*}{\sin^2\xi_*} \tag{2.2}$$

where $\hat{q}_v$, $\overline{U}$, n are parameters of load, horizontal stress resultant and eccentricity of shell respectively, $\xi = (\psi_0 - \xi_0)/\varepsilon$, ξ_0 is the angle defining location of the inner boundary layer (Fig. 1), ψ_0 is the angle coordinate of the shell point.

Considering isotropic spherical shell under uniform external pressure and introducing change of variables

$$\psi = \gamma - g_0, \quad \gamma = \xi_0, \quad f_0 = \overline{U}\sin\xi_0, \quad \hat{q}_v = 2\lambda_0\sin\gamma, \quad \lambda_0 = q/q_* \tag{2.3}$$

we arrive to the limiting equations

$$\ddot{g}_0 = -f_0\frac{\sin(\gamma - g_0)}{\sin\gamma} - 2\lambda_0\cos(\gamma - g_0)\sin\gamma \tag{2.4}$$

$$\ddot{f}_0 = \frac{\cos(\gamma - g_0) - \cos\gamma}{\sin\gamma} \tag{2.5}$$

obtained earlier in Kriegsmann and Lange (1980). It is also shown in this paper that $\lambda_0 = 0$ for the completed sphere as well as in the case, when boundary layer region is located sufficiently far from the shell edge. If the boundary layer region is located close to the shell edge (fully inverted shell), $\lambda_0 \sim 1$ or respectively $\hat{q}_v \sim 1$ in Eqs. (2.1) and (2.2).

We will consider classical boundary conditions, which in the first order of asymptotic approximation according to Eqs. (3.32)–(3.34) of Part 1 could be represented as follows:

$$\psi = \xi_*, \qquad \overline{U}' - \frac{n}{\sin\xi_*}\psi' = 0 \tag{2.6}$$

$$\psi = \xi_*, \qquad \overline{U} = 0 \tag{2.7}$$

$$\psi' + n\sin\xi_*\overline{U}' = 0, \qquad \overline{U}' - \frac{n}{\sin\xi_*}\psi' = 0 \tag{2.8}$$

The first condition corresponds to the clamped edge of the shell, the second condition corresponds to an edge resting on a frictionless surface, and the last one is the simply supported edge.

The considered boundary value problems are free of singularities and contain only two parameters: n and ξ_*. Solving them by applying standard numerical methods, one can obtain equilibrium paths as well as strain and stress states of shell with large deflections. The samples of such solutions for composite shallow spherical caps under uniform external pressure are given below.

We simplify the boundary value problems by introducing approximations

$$\sin x \approx x, \quad \cos x \approx 1 - 0.5x^2 \tag{2.9}$$

which correspond to the technical shell theory containing only quadratic nonlinear terms. After changing of variables

$$\overline{U} = 2\varphi_0, \quad \psi = \xi_0(1 - 2w_0) \tag{2.10}$$

we arrive at the equations

$$w_0'' - n\varphi_0'' - \varphi_0(1 - 2w_0) + q_0 = 0 \tag{2.11}$$

$$\varphi_0'' + nw_0'' - w_0(1 - w_0) = 0 \tag{2.12}$$

with one of the following boundary conditions (at $\xi = \xi_1$)

$$w_0 = 0, \qquad \varphi_0' + nw_0' = 0 \tag{2.13}$$

$$w_0 = 0, \qquad \varphi_0 = 0 \tag{2.14}$$

$$w_0' - n\varphi_0' = 0, \qquad \varphi_0' + nw_0' = 0 \tag{2.15}$$

and

$$w_0 = 1, \quad \varphi_0 = q_0 \quad \text{at } \xi \to -\infty \tag{2.16}$$

These boundary value problems for shallow composite shells contain only one structural parameter n, which is equal to zero for any shells symmetrical about their midsurfaces, or for ones having eccentricity only in the circumferential direction.

Formulae (3.37)–(3.39) of Part 1 for bending moments and main stress resultant take the form:

$$M_1 = \frac{2D\sqrt{W_0}}{\varepsilon R^{3/2}}(n\varphi_0' - w_0'), \quad M_2 = \frac{2D\sqrt{W_0}}{\varepsilon R^{3/2}}(n^*\varphi_0' - D^*w_0') \tag{2.17}$$

$$N_2 = \frac{2D^{1/4}(a_*B_{22})^{3/4}\sqrt{W_0}}{R}\varphi_0' \tag{2.18}$$

where W_0 is deflection amplitude.

The results of numerical solutions are represented in Figs. 1–4. We introduce the parameter $C_* = (\xi_* - \xi_0)/\varepsilon$, which characterizes the closeness of the inner boundary layer to the edge of the shell. In the case of shallow spherical shell we have $\xi_* = (2H/R)^{1/2}$ and $\xi_0 = (W_0/R)^{1/2}$, and therefore

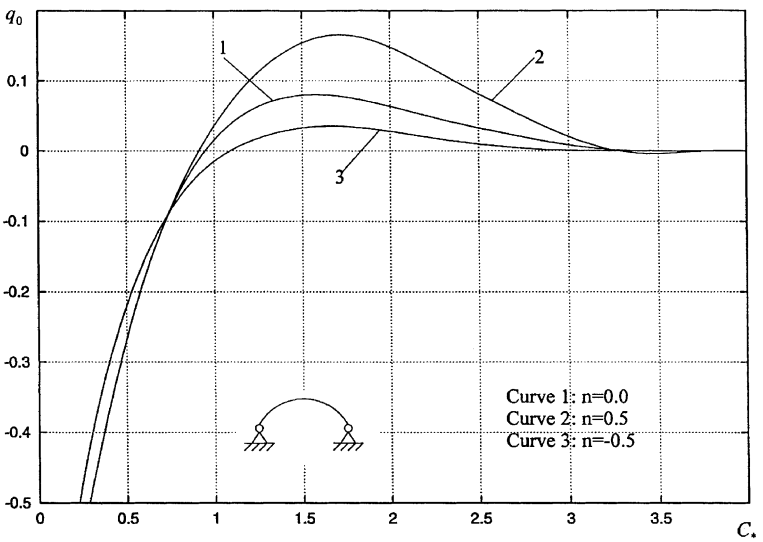

Fig. 2. Load parameter versus deflection amplitude of simply supported composite cap.

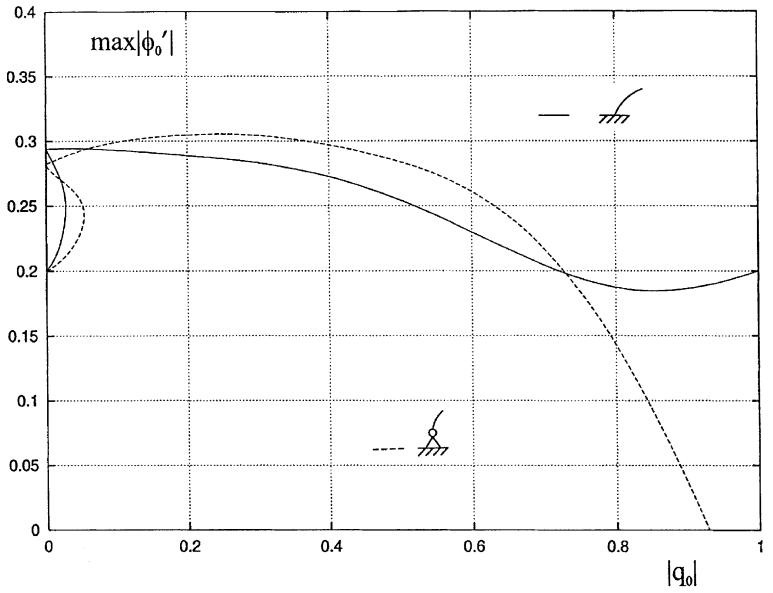

Fig. 3. Parameter of maximum circular membrane stresses of inverted spherical shells.

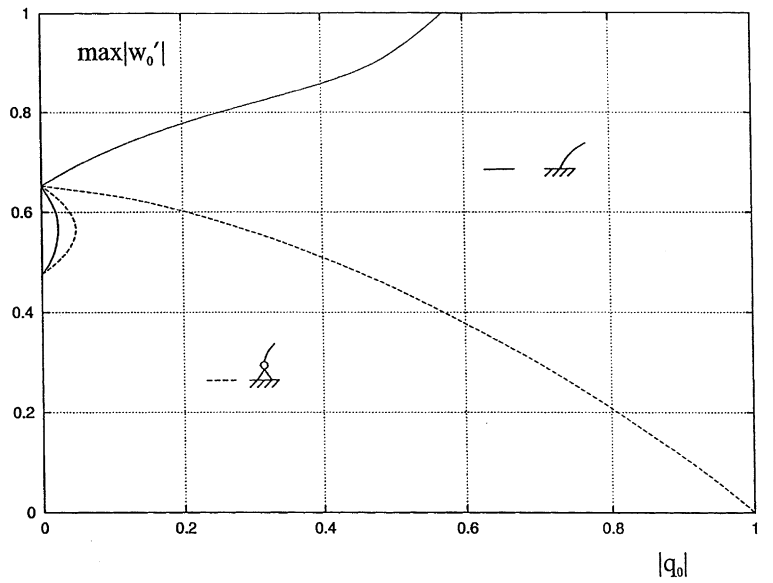

Fig. 4. Parameter of maximum bending stresses of inverted spherical shells.

$$C_* = \frac{\sqrt{2H} - \sqrt{W_0}}{\varepsilon\sqrt{R}} \tag{2.19}$$

The relations between load parameter q_0 and parameter C_*, which characterizes deflection amplitude on account of the shell inversion, are shown in Figs. 1 and 2. Parameter $C_* = 0$, if the deflection amplitude of shell reaches $2H$, where H is the rise of the cap.

The behavior of shell with different boundary conditions changes when C_* tends to 0 (fully inverted shell). The external pressure dramatically increases for the case of clamped shell while it changes from positive to negative for the simply supported shell. The structure behavior changes slightly with variation of eccentricity parameter n, including its sign. Load parameter $q_0 \approx 0$ for relatively large C_* ($C_* \geqslant 4$ for the clamped shell and $C_* \geqslant 3$ for the simply supported one), which corresponds to the location of boundary layer sufficiently far from the edge of the shell. We will consider this case in the next section.

The plots of maximum values of functions $\max|\varphi_0'|$ and $\max|w_0'|$, which correspond (according to formulae (1.17) and (1.18)) to the maximum values of membrane and bending stresses respectively, are shown in Figs. 3 and 4 for two types of boundary conditions (here $n = 0$). Comparison of Figs. 3 and 4 and Figs. 1 and 2 shows that the membrane and bending stresses vanish as a simply supported sphere becomes fully inverted ($C_* \to 0$, $W_0 \to 2H$, $|q_0| \sim 1$). Oppositely, by inverting clamped shell the bending stresses ($\max|w_0'|$) sharply increase while the membrane ones change slightly ($\max|\varphi_0' \approx 0.2|$). It should be noted that considered functions describe only additional boundary layer stresses. The membrane and bending stresses in the main inverted part of shell could be easily calculated.

3. Orthotropic ellipsoid of revolution with large deflections

In the case of completed shell or if the inner boundary layer is located far enough from the shell edge it is not necessary to solve equations in order to obtain simple asymptotic formulae describing behavior of the structure subject to a changing load, as well as to evaluate main stress components. It is sufficient to use the asymptotic variational relationship (3.69) of Part 1 in the form

$$\frac{\partial W_1}{\partial \xi_0} = \frac{\partial A_1}{\partial \xi_0} \tag{3.1}$$

where W_1 is the deformation energy of shell within the inner boundary layer region and it can be evaluated using asymptotic formula (3.42) of Part 1

$$W_1 = a_* \pi B_{22} R_1^3 \xi_0^2 \sin\xi_0 \varepsilon^3 J/R_2, \quad J = 2.23 + 0.116\xi_0^2 \tag{3.2}$$

In order to illustrate the suggested approach we will consider two types of loading: uniform external pressure and concentrated force. The variation of the work A_1 of pressure q can be represented as follows

$$\frac{\partial A_1}{\partial \xi_0} = 2\pi q R_2^2 \sin^2\xi_0 \frac{\mathrm{d}z(\xi_0)}{\mathrm{d}\xi_0} \tag{3.3}$$

where $z = z(\psi_0)$ and $r_0 = r_0(\psi_0)$ are parametrical equations of midsurface of shell of revolution. For the transversal force Q applied in the shell pole we have $A_1 = QW_0$,

$$W_0 = 2[z(\xi_0) - z(0)] \quad \text{and} \quad \frac{\partial A_1}{\partial \xi_0} = 2Q\frac{\mathrm{d}z(\xi_0)}{\mathrm{d}\xi_0} \tag{3.4}$$

where W_0 is the deflection of the shell pole.

As an example we will consider the shell with a midsurface in a shape of an ellipsoid of revolution given by equation

$$\frac{r_0^2}{b^2} + \frac{z^2}{c^2} = 1 \tag{3.5}$$

where b and c are the semi-axes of the ellipsoid. Let us assume that their ratio $\lambda = c/b \leqslant 1$. Then the largest radius of curvature of the shell $R_* = b/\lambda$ will be attained at $r_0 = 0$, i.e., on the minor axis of the ellipsoid, which is its axis of rotation.

We apply also the geometrical relations for the ellipsoid of revolution

$$R_2 = R_*\gamma_*^{1/2}, \quad R_1 = R_*\gamma_*^{3/2}, \quad \gamma_* = \frac{1+\tan^2\xi_0}{1+(\tan^2\xi_0)/\lambda^2}, \quad z = \lambda^2\frac{r_0}{\tan\psi_0} \tag{3.6}$$

$$r_0 = \frac{R_*\tan\psi_0}{\left(1+\frac{\tan^2\psi_0}{\lambda^2}\right)^{1/2}}, \quad W_0 = 2c\frac{\sqrt{\lambda^2+\tan^2\xi_0}-\lambda}{\sqrt{\lambda^2+\tan^2\xi_0}} \tag{3.7}$$

then according to Eq. (3.2) the expression for the deformation energy takes the form

$$W_1 = a_*\pi B_{22}R_*^2\xi_0^2\sin\xi_0\varepsilon_*^2\gamma_*^{1/4}J(\xi_0) \tag{3.8}$$

where

$$\varepsilon_*^2 = (1/R_*)(D_{11}/a_*B_{22})^{1/2} \tag{3.9}$$

Instead of Eq. (3.3) we obtain the following formula after a simple rearrangement in the case of uniform external pressure q

$$\frac{\partial A_1}{\partial\xi_0} = 2\pi qR_*^3\sin^3\xi_0\gamma_*^{5/2} \tag{3.10}$$

Varying the total potential energy over ξ_0 according to Eq. (3.1) and assuming that parameter of eccentricity $n = 0$ we finally arrive at the expression for the external pressure parameter

$$\bar{q} = \varepsilon_*\frac{T(\xi_0,\lambda)}{8} \tag{3.11}$$

where $\bar{q} = q/q_*$

$$q_* = 4/R_*^2\sqrt{a_*D_{11}B_{22}} \quad \text{and} \quad T(\xi_0,\lambda) = \frac{J(4\tan\xi_0+\xi_0(1+\gamma_*))\xi_0+2\xi_0^2\tan\xi_0\frac{\mathrm{d}J}{\mathrm{d}\xi_0}}{2\sin^2\xi_0\tan\xi_0\gamma_*^{9/4}} \tag{3.12}$$

Formulae (3.11) and (3.12) together with Eq. (3.7) give the necessary link between load and deflection amplitude W_0. The post-buckling equilibrium paths obtained from these formulae are shown in Fig. 5 for different values of ratio λ. If $\lambda = 1$, which corresponds to the complete spherical shell, our solution coincides with the obtained for the isotropic sphere (Graff et al., 1985). The both solutions are also in a good agreement with known numerical studies, in which the full Reissner's equations were used. More detailed comparison of asymptotic results with numerical ones both in post-buckling behavior and stress states of spherical shells is described in Evkin and Korovaitsev (1992), Korovaitsev and Evkin (1992) and Evkin (1995).

We note that each curve in Fig. 5 has a minimum value of load parameter, which restricts the domain of existence of equilibrium configuration. For this value, which is important in analysis of shell stability, we obtain the following expression:

$$\bar{q}_{\min} = \frac{T_{\min}(\lambda)}{8}\varepsilon_* \tag{3.13}$$

Solid line in Fig. 6 represents a plot of the function $\bar{q}_{\min}/\varepsilon$. This function could be slightly simplified when parameter λ is small. Numerical investigation of formula (3.12) shows that the function (3.12) reaches its minimum at small ξ_0, when λ is small as well, therefore we can assume that $\xi_0^2 \ll 1$ for $\lambda \leqslant 0.5$. Then expression (3.12) can be represented in the form

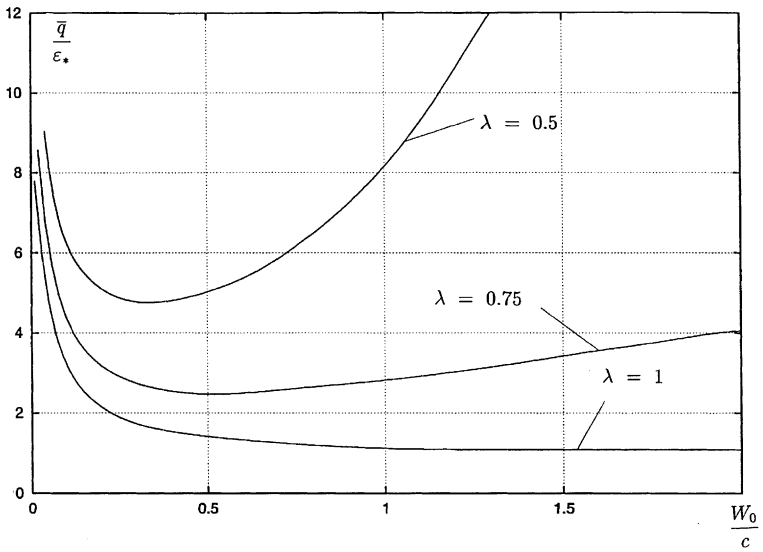

Fig. 5. Load–displacement diagrams of orthotropic ellipsoids of revolution.

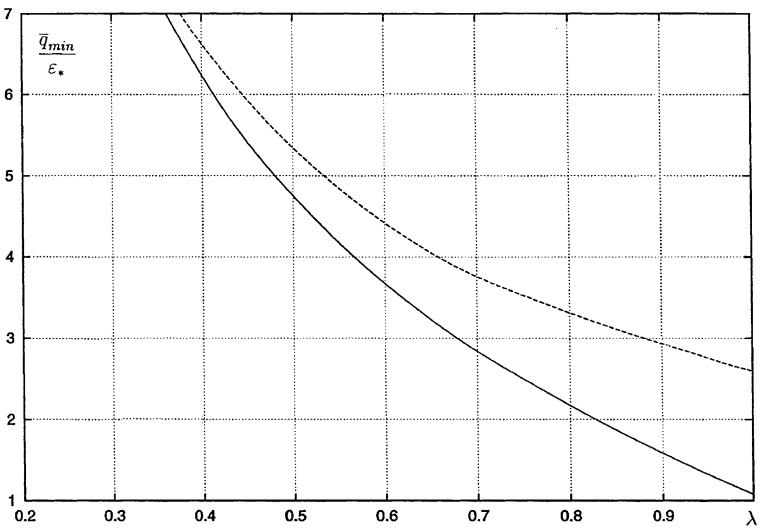

Fig. 6. Minimum load parameter depending on ratio of the ellipsoid axes.

$$T(x_*, \lambda) = \frac{(6 + 5x_*^2)(1 + x_*^2)^{5/4}}{2x_*\lambda} J_0, \quad x_* = \xi_0/\lambda, \quad J_0 = 2.23 \tag{3.14}$$

Finding the minimum of Eq. (3.14) for the variable x_* we obtain

$$T_{\min} = 21.2/\lambda \quad \text{at } x_* \approx 0.55 \tag{3.15}$$

Then the expression for the minimum pressure parameter takes the form

$$\bar{q}_{\min} = \frac{2.65}{\lambda}\varepsilon_* \tag{3.16}$$

or for isotropic ellipsoid, assuming Poisson's ratio $\nu = 0.3$,

$$\bar{q}_{\min} = \frac{1.46}{\lambda}\sqrt{\frac{h}{R_*}} \tag{3.17}$$

It follows from last formula that $\bar{q}_{\min}$ increases with decreasing λ. For example, for $R_*/h = 100$ and $\lambda = 0.25$ we have $\bar{q}_{\min} = 0.58$, however $\bar{q}_{\min}$ decreases with decreasing thickness ratio of the shell. The approximate formula (3.16) is plotted in Fig. 6 by dashed line.

For the case of concentrated load Q it is easy to obtain the relation

$$\overline{Q} = \lambda^2\gamma_*^{5/2}\left(\cos^2\xi_0 + \frac{\sin^2\xi_0}{\lambda^2}\right)^{3/2}\sin^2\xi_0 T(\xi_0,\lambda) \tag{3.18}$$

where $\overline{Q} = (2\lambda^2 Q)/(\pi\varepsilon_*(a_* B_{22} D_{11})^{1/2})$. Formula (3.18) together with Eq. (3.7) gives the relations between load parameter and the deflection amplitude W_0. They are shown in Fig. 7 for different values of parameter λ. We can observe the different types of essentially nonlinear behavior of shells with large deflections. If $\lambda = 1$ we have the case of completed orthotropic spherical shell. If the angle ξ_0 is not large we can assume that $\sin\xi_0 \approx \xi_0$, and $\cos\xi_0 \approx 1 - \xi_0^2/2$. In this case we obtain a simple formula

$$\overline{Q} = 3J_0\xi_0 = 3J_0\sqrt{\frac{W_0}{R}}$$

which coincides with the results in Pogorelov (1967) and Ranjan and Steele (1977) derived by using geometrical-energy method for large deflection of the isotropic spherical shell. In the last study the obtained formula was also expanded to the small deflections.

It is easy to generalize the formula (3.18) for the case of combination of both concentrated force and external uniform pressure. We have obtained the following relation

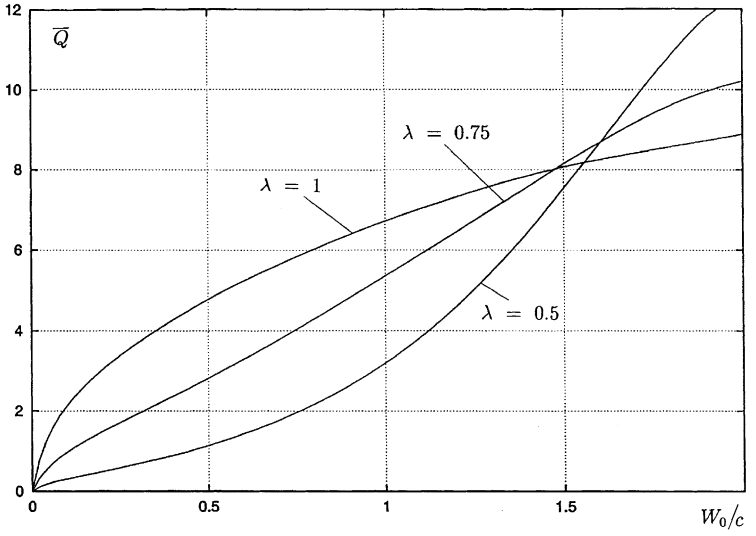

Fig. 7. Parameter of concentrated load depending on deflection amplitude of orthotropic ellipsoids of revolution.

$$\overline{Q} = \lambda^2 \gamma_*^{5/2} \left(\cos^2 \xi_0 + \frac{\sin^2 \xi_0}{\lambda^2} \right)^{3/2} \sin^2 \xi_0 \left[T(\xi_0, \lambda) - \frac{8\bar{q}}{\varepsilon_*} \right] \tag{3.19}$$

Corresponding results are shown in Figs. 8–10. In Fig. 8 the equilibrium paths of spherical shell under changing concentrated force and constant pressure of different levels are represented. The curves 1–4 correspond to the following four values of the pressure parameter $(\bar{q}/\varepsilon_*) = 0, 0.5, 0.8, 1.07$ respectively. The last value 1.07 coincides with the minimum pressure according to the formula (3.13). Such additional pressure is sufficient to change significantly the behavior of the shell under concentrated load. The curves 1–3 shown in Figs. 9 and 10, correspond to the values of the pressure parameter $(\bar{q}/\varepsilon_*) = 0$, 3.6, 4.65 for orthotropic ellipsoid of revolution with geometrical parameter $\lambda = 0.5$. The last value 4.65 coincides with the minimum external pressure according to formula (3.13). Figs. 9 and 10 represent the same results, but in Fig. 9 we are focused on the interval $W_0 \geqslant 1.5c$ and in Fig. 10 we show behavior of the shell for $W_0 \leqslant c$. We consider two domains of displacement W_0 with different types of shell behavior. The first one ($W_0 \geqslant 1.5c$) is characterized by a slight influence of the additional external pressure (Fig. 9). In the second region ($W_0 \leqslant c$) we observe the significant impact of additional pressure with maximum and minimum values on the curve 3 in Fig. 10.

It should be noted that the suggested approach and the obtained formulae are applicable only for large deflections. Therefore we restricted ourselves by consideration of small additional external pressure avoiding the consideration of a stability problem for spherical shell under external pressure. In order to solve the stability problem we should expand the results to the area of small deflections. This direction has been outlined in Evkin (1989), where also a practical estimation of validity domain ($W_0 \geqslant 5h$, where h is the shell thickness) of the suggested approach has been obtained in the case of isotropic shells.

Finally, we obtain the following expressions:

$$\max |M_1| = \frac{D_{11}\xi_0}{\gamma_*^{1/4} R_* \varepsilon_*} \max |\varphi'|, \quad \max |M_2| = \frac{D_{21}}{D_{11}} \max |M_1| \tag{3.20}$$

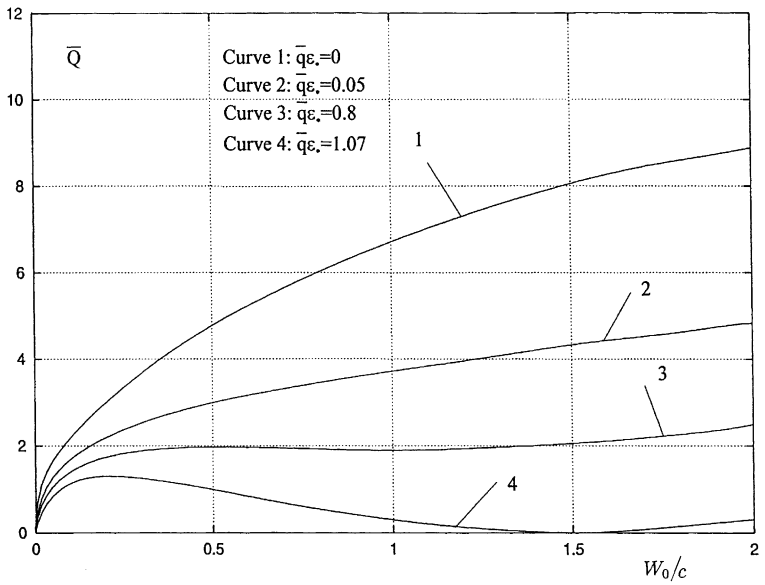

Fig. 8. Behavior of spherical shell under combination of loads: external pressure and concentrated load.

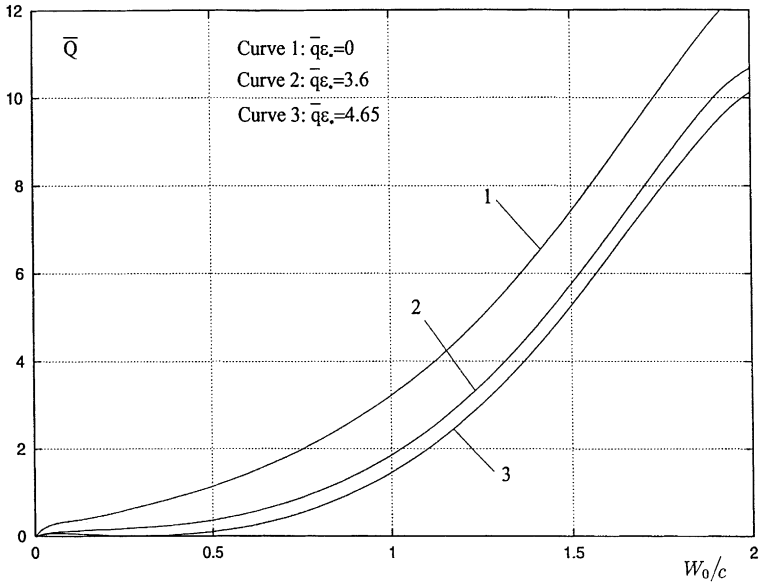

Fig. 9. Load–displacement diagram of orthotropic ellipsoid of revolution ($\lambda = 0.5$) under combined loading of external pressure and concentrated load.

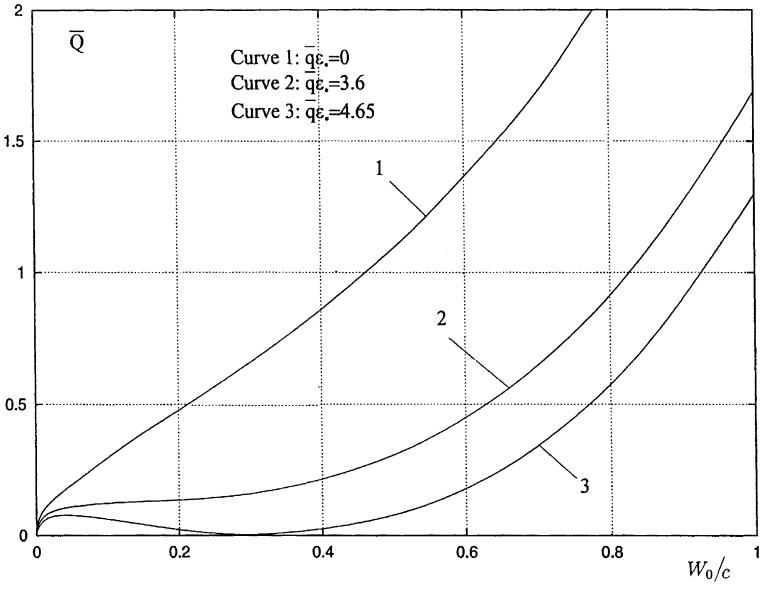

Fig. 10. Nonlinear behavior of ellipsoid of revolution ($\lambda = 0.5$) under combined load of external pressure and concentrated load.

$$\max |N_2| = a_* B_{22} \xi_0 \varepsilon_* \max |f| / \gamma_*^{1/4} \tag{3.21}$$

which could be useful for evaluation of extreme stress values. For example, Fig. 11 shows the change of the stress state with the increase of deflection amplitude. Here curves 1 and 1′ correspond to the maximum

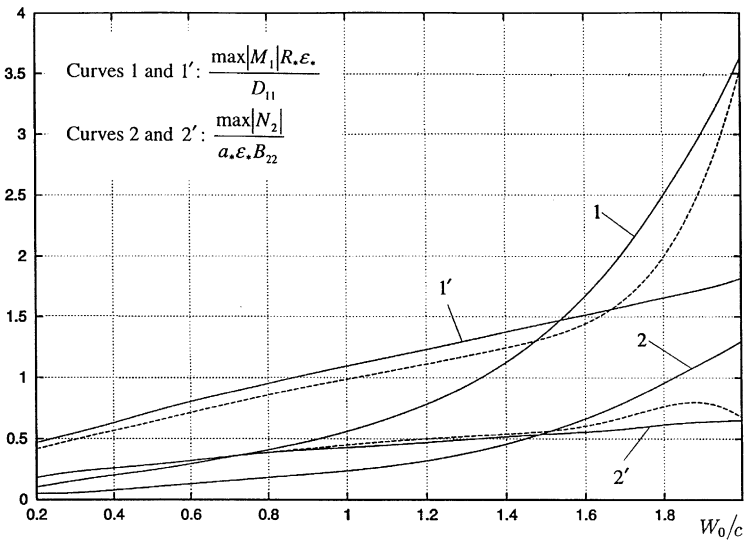

Fig. 11. Maximum bending moment and stress resultant depending on deflection amplitude of ellipsoids of revolution.

bending moment, curves 2 and 2′ correspond to the maximum membrane stress resultant. The results are represented for ellipsoid of revolution with parameter $\lambda = 0.25$ (curves 1 and 2) and for spherical shell (curves 1′ and 2′) under uniform external pressure. In the last case we compare asymptotic solution with numerical one (dashed lines), obtained in Evkin and Korovaitsev (1992) for the isotropic hemisphere with rigidly clamped edge and with parameters $R/h = 100$, $\nu = 0.3$. There is a good agreement of results in the considered range of deflection amplitude, except when $W_0/R \approx 2$. The difference between two solutions seems to be natural in this narrow region, because of the influence of boundary condition considered in the numerical solution. It is different from conditions taken into account in the analytical solution, which correspond to a completed sphere. It is worth to note that the formulae (3.20) and (3.21) as well as plots shown in Fig. 11 do not depend on type of loading but they depend only on the value of the deflection amplitude W_0.

4. Conclusions

The numerical solution of asymptotic boundary value problems, which have been derived in Part 1 of this study (Evkin and Kalamkarov, 2001), demonstrates different types of behavior of shell with large axially symmetric deflections. It is shown that the boundary conditions play a crucially important role in the case of fully inverted shell, when inner boundary layer is close to the shell edge. For example, a strong increase of external pressure has been obtained for the clamped shell, in contrast to the simply supported shell when the pressure changed from positive to negative. It is interesting that the variation of value and sign of structure eccentricity parameter n slightly impacts the behavior diagram with large deflections of composite shells, except region with small values of external pressure.

The consideration of completed shells, for example orthotropic ellipsoids of revolution, allows us to make the conclusion that the pressure parameter takes asymptotically small value for large deflections and it can reach a minimum of a magnitude depending on variation of the geometrical and stiffness parameters of the shell in meridian direction. This minimum can be used for estimation of lower limit of pressure for the existence of post-buckling axially symmetric equilibrium configuration of the shell of revolution.

Finally, we are able to conclude that the asymptotic relations obtained in Part 1 of this study can be successfully used in the analyses of both load–displacement diagrams for different types of shells of revolution and their stress states.

Acknowledgements

This work has been supported by the Natural Sciences and Engineering Research Council of Canada.

References

Evkin, A.Yu., 1989. A new approach to the asymptotic integration of the equations of shallow convex shell theory in the post-critical stage. Prikl. Matem. Mekh. (PMM) 53 (1), 115–120 (English translation: J. Appl. Math. Mech. 53 (1) (1989) 92–96).

Evkin, A.Yu., 1995. Large deflections of thin shells: asymptotic solutions. Proc. 15th Can. Cong. Appl. Mech. 1, 284–285.

Evkin, A.Yu., Kalamkarov, A.L., 2001. Analysis of large deflection equilibrium states of composite shells of revolution. Part 1: General model and singular perturbation analysis. Int. Journal of Solids and Structures.

Evkin, A.Yu., Korovaitsev, A.V., 1992. Asymptotic analysis of the transcritical axisymmetric state of stress and strain in shells of revolution under strong bending. Izv. Ross. Akad. Nauk, Ser. Mekhanika Tverdogo Tela 27 (1), 125–133 (English translation: Bull. Rus. Acad. Sci./ Mech. Solids 27 (1) (1992) 121–129).

Graff, M., Scheidl, R., Troger, H., Weinmuller, E., 1985. An investigation of the complete post-buckling behavior of axisymmetric spherical shells. J. Appl. Math. Phys. (ZAMP) 36, 803–821.

Korovaitsev, A.V., Evkin, A.Yu., 1992. Axisymmetric deformation of toroidal shells with strong flexure. Prikladnaya Mekhanika 28 (4), 16–23 (English translation: International Applied Mechanics, 28 (4) (1992) 216–222).

Kriegsmann, G.A., Lange, C.G., 1980. On large axisymmetrical deflection states of spherical shells. J. Elast. 10, 179–192.

Pogorelov, A.V., 1967. Geometrical methods in nonlinear theory of elastic shells. Nauka, Moscow, in Russian.

Ranjan, G.V., Steele, C.R., 1977. Large deflection of deep spherical shells under concentrated load. Proceedings, AIAA J/ASME 18th Structures, Structural Dynamics, and Materials Conference, San Diego, California, Tech. Paper No. 77-411, pp. 269–278.

Reissner, E., 1969. On finite symmetrical deflections of thin shells of revolution. J. Appl. Mech. 36, 267–270.

Reissner, E., 1972. On finite symmetrical strain in thin shells of revolution. J. Appl. Mech. 39, 1137–1138.